Metal oxides for thermochemical energy storage – From gas-triggered isothermal cycling to low-temperature applications with increased O_2 pressure

Christian Knoll,[1,2] Georg Gravogl[1,3], Werner Artner,[4] Elisabeth Eitenberger,[5] Gernot Friedbacher,[5] Andreas Werner,[6] Ronald Miletich,[3] Peter Weinberger,[1] Danny Müller,[1]* Michael Harasek[2]

[1] Institute of Applied Synthetic Chemistry, TU Wien, Getreidemarkt 9/163-AC, 1060 Vienna, Austria

[2] Institute of Chemical, Environmental & Biological Engineering, TU Wien, Getreidemarkt 9, 1060 Vienna, Austria

[3] Institut für Mineralogie und Kristallographie, University of Vienna, Althanstraße 14, (UZA 2), 1090 Vienna, Austria

[4] X-Ray Center, TU Wien, Getreidemarkt 9, 1060 Vienna, Austria

[5] Institute of Chemical Technologies and Analytics, TU Wien, Getreidemarkt 9/164, 1060 Vienna, Austria

[6] Institute for Energy Systems and Thermodynamics, TU Wien, Getreidemarkt 9/302, 1060 Vienna, Austria

danny.mueller@tuwien.ac.at

Abstract

Metal oxides providing various, reversibly accessible oxidation states are in the focus as auspicious materials for high-temperature thermochemical energy storage (TCES) materials. Among all principally suitable metal oxides due to equilibrium temperature and, in particular, reaction rate and reversibility, only the couple Co_3O_4 / CoO and to a smaller extend Mn_2O_3 / Mn_3O_4 are considered as suitable candidates. Based on recent studies on isothermal TCES-cycles, the impact of temperature and increased O_2-pressure on the reaction rate was investigated by varying the O_2-partial pressure in the low-temperature oxidation of the reduced oxide. Whereas Mn_3O_4 was found to react too slow for a process at lower temperatures, CoO was found suitable. For an increase of the O_2 pressure to 6 bar between 500 – 550 °C an attractive oxidation behavior was observed. At 900 °C Co_3O_4 / CoO could be cycled within 4.5 minutes between both oxidation states by changing the atmosphere from N_2 to O_2 and vice versa.

Keywords: cobalt oxide, manganese oxide, non-ambient pressure, in-situ powder X-Ray diffraction, thermochemical energy storage

1. Introduction

The different technologies suitable for thermal energy storage are defined according to the storage process as sensible (Dinker et al., 2015), latent (Zalba et al., 2003) and thermochemical heat storage (Abedin, 2011; Cot-Gores et al., 2012). The latter provides the highest storage densities and has the potential for loss-less storage, once the material was charged. The necessary smaller amounts of material – related to the higher storage densities compared to other techniques, – as well as the enormous applicational flexibility due to the large temperature range being tolerated, are additional advantages of this technique. (Yan, 2015)

The loss-less storage ability of thermochemical energy storage materials (TCES-materials) is an intrinsic feature, as no discharging of the storage occurs in the absence of the reactive gas. The broad operational temperature

doi:10.18086/swc.2017.14.02 Available at http://proceedings.ises.org

profile of TCES-materials is given by the equilibrium temperatures of the applied substance classes. By ranking the materials following to the involved reactive gases such as H_2O, NH_3, H_2, CO_2 or O_2, the field of application for TCES-materials ranges from low-temperature storage with temperatures below 100 °C (van Essen et al., 2009; Knoll et al., 2017) (mostly hydrated salts for *e.g.* civil engineering applications as in an energy self-sufficient building) to medium-temperature storage using ammoniates or hydrides and to temperatures between 800-1200 °C (T. Yan, 2015), using carbonates or oxides in combination with *e.g.* concentrating solar power plants. (Pardo et al., 2014)

Oxides suitable for TCES require several stable oxidation states of the metal, reversibly accessible via redox-reactions. During the charging of the storage material the metal is reduced, while discharging in the presence of O_2 leads to a restorage of the (initial) higher oxidation state (see equation 1).

$$M_xO_{y+n} + \Delta H \leftrightarrow M_xO_y + \frac{n}{2} O_2 \quad (1)$$

Although, metal oxides are investigated with respect to their thermochemical properties since the 80's, only a few suitable oxides are known due to the necessary reversibility of the redox-process. Candidate materials promising for application are the couple Co_3O_4 / CoO, as well as Mn_2O_3 / Mn_3O_4 considering reversibility, toxicity issues, temperature range and reaction time. A variety of studies was reported in particular for the cobalt system, covering cycle stability tests (Agrafiotis et al., 2014), composite materials, (Agrafiotis et al., 2016a), (Agrafiotis et al., 2015a; 2015b; Karagiannakis et al., 2016) materials optimization via spinel-phases (Babiniec et al., 2015; Block et al., 2014; LiuPrewitt, 1990), mechanical stress (Karagiannakis et al., 2016), etc. Although, Mn_2O_3 is also widely known for TCES purposes, (Carrillo, A. J. et al., 2014) due to the slower reaction kinetics, (Alonso et al., 2013; Chen et al., 2013) as well as the minor performance compared to the cobalt-system. Most efforts focussed on the dotation of Mn_2O_3 with iron (Carrillo, A. J. et al., 2015;Wokon et al., 2017), forming perovskites, or the combination with Co_3O_4 for a combined system. (Agrafiotis et al., 2016b)

Theoretically suitable metal oxides such as ZnO, (Palumbo, 2001) Fe_2O_3 or V_2O_5 feature equilibrium temperatures well above 1500 °C (Pardo et al., 2014), hampering both their routine investigation for storage processes, and their combination with conventional concentrating solar power plants. In order to expand the portfolio of redox-TCES materials, experimental approaches combining TCES with syngas production (Muthusamy et al., 2014), or the application of peroxide / oxide reactions (Carrillo, A. J. et al., 2016) were reported for energy storage in literature.

Apart from their potential of bridging non-operational times in concentrating power plants, the interest in oxidic TCES-materials relates mainly to their high storage density. Recently we could demonstrate (Müller et al., 2017), that between 830 - 930 °C a regime of coexistence between CoO and Co_3O_4, depending on the O_2-concentration, allows for isothermal TCES-cycles. Moreover, both CoO and Mn_3O_4 start oxidation under O_2-atmosphere already below 500 °C. Materials of high storage densities would be highly appreciated for applications around these temperatures. To enhance the reaction rate and obtain a material, which would combine fast reaction rates with high energy densities and a broad perspective of applicability, in the present study the impact of temperature on the isothermal redox-cycle, and the effect of an increased oxygen partial pressure on the oxidation rate was investigated by an *in-situ* powder diffraction (P-XRD) study.

2. Experimental

2.1 Material

Cobalt(II,III) oxide (99.995%), cobalt(II) oxide (99.99%), manganese(IV) oxide (99.99%) and manganese(II, III) oxide (97%) were obtained from Sigma-Aldrich and used as supplied.

2.2 X-Ray Powder Diffraction

The powder X-ray diffraction measurements were carried out on a PANalytical X'Pert Pro diffractometer in Bragg-Brentano geometry using Cu $K_{\alpha1,2}$ radiation and an X'Celerator linear detector with a Ni-filter. For *in-situ* experiments at elevated pressures an Anton Paar XRK 900 reaction chamber, operable between ambient pressure and 12 bar was used. The sample was mounted on a hollow ceramic powder sample holder, allowing for complete perfusion of the sample with the reactive gas. The sample temperature is controlled directly via a NiCr-NiAl thermocouple and direct environmental heating. For the *in-situ* experiments at ambient pressure an Anton Paar HTK 1200N sample chamber was used. The sample temperature is controlled via a Pt 10 % RhPt thermocouple and direct environmental heating. The diffractograms were evaluated using the PANalytical program suite HighScorePlus v4.6a. (Degen et al., 2014) A background correction and a $K_{\alpha2}$ strip were performed. Phase assignment is based on the ICDD-PDF4+ database ((http://www.icdd.com), the exact phase composition, shown in the conversion plots, was obtained via Rietveld-refinement incorporated in the program suite HighScorePlus v4.6a. (Degen et al., 2014) All quantifications based on P-XRD are accurate within of ±5 %.

2.3 Thermal Analysis

For thermal analysis of the redox-reactions a Netzsch TGA/DSC 449 C Jupiter ® equipped with a water vapour furnace including an air-cooled double jacket was used. The oven operates between 25 °C and 1250 °C, regulated by an S-type thermocouple. Oxygen and nitrogen gases were 99.999 % and obtained from Messer. For all measurements under air a mixture of 21 % O_2 and 79 % N_2 was applied. The gas flow was set to 25 ml min^{-1}, controlled and mixed with Vögtlin Instruments "red-y" mass flow controllers. A sample mass of 20 mg in an open Al_2O_3 crucible was used for all experiments with heating and cooling rates of 10 °C min^{-1}. The DSC was calibrated according to the procedure suggested by Netzsch, using the In, Sn, Bi, Zn, Al and Ag standards provided by the manufacturer.

2.4 Scanning Electron Microscopy

SEM images were recorded on gold coated samples with a Quanta 200 SEM instrument from FEI under low-vacuum at a water vapor pressure of 80 Pa to prevent electrostatic charging.

3. Results and Discussion

3.1 Isothermal oxidation of CoO triggered by variation of the reactive gas

Based on the previously identified window of coexistence between CoO and Co_3O_4, selected temperatures between 880 °C and 920 °C were chosen to determine the reaction rate by isothermal thermogravimetry / differential scanning calorimetry (TG / DSC). The isothermal reduction of Co_3O_4 under N_2 with subsequent oxidation by changing the atmosphere to O_2[*] was investigated at five temperature levels for each two cycles (figure 1).

[*] The redox-reaction of Co_3O_4 under gas-change conditions was confirmed to be highly comparable for 20 consecutive cycles (figure S1).

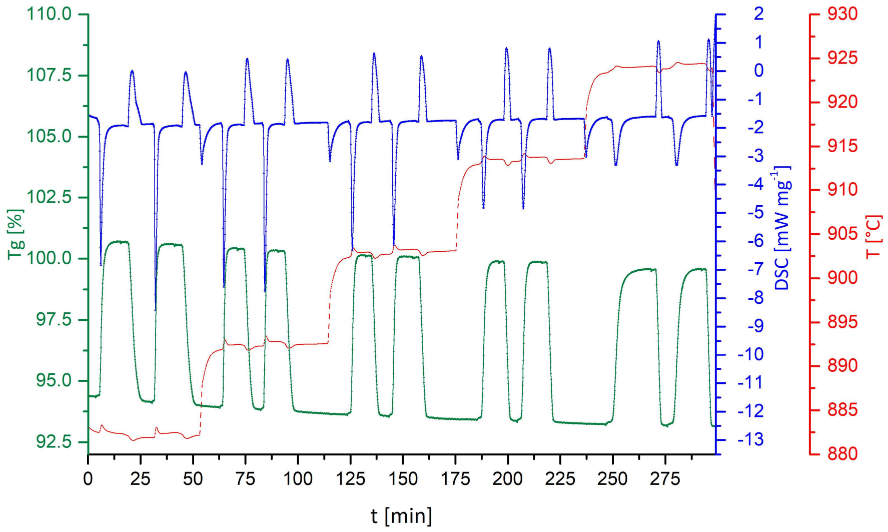

Fig. 1: TG / DSC of isothermal redox-cycles of Co_3O_4, triggered by variation of the atmosphere at 880, 890, 900, 910 and 920 °C. Reduction occurs under N_2-atmosphere, oxidation under O_2-atmosphere.

The averaged reaction times for reduction and oxidation, obtained from figure 1, are given in table 1.

Tab. 1: Average reaction times for isothermal reduction of Co_3O_4 (under N_2) and oxidation of CoO (under O_2), calculated from the differential scanning calorimetry data

	880 °C	890 °C	900 °C	910 °C	920 °C
Oxidation [min]	3.92 ± 0.40	3.35 ± 0.03	4.54 ± 0.11	4.95 ± 0.03	6.91 ± 0.28
Reduction [min]	7.07 ± 0.15	5.58 ± 0.05	4.62 ± 0.08	3.96 ± 0.08	3.41 ± 0.19

Except the spike for the oxidation time at 890 °C, an apparent linear correlation between reaction time and temperature is obtained. The oxidation time doubles with increased isothermal temperature almost nearly over the whole investigated temperature range, whereas the reduction time is exactly halved. Based on the herein obtained results the most suitable temperature for such an isothermal TCES-process is identified with 900 °C, where oxidation and reduction of the material are taking equal times.

The presented isothermal redox-cycling between 880 - 920 °C with the optimum at 900 °C represents a notable improvement regarding the earlier investigations, where oxidation was accomplished within 10.4 minutes at 848 °C and the complete reduction accounted for 23 minutes. (Müller et al., 2017)

3.2 Isothermal oxidation of CoO

The second objective of the current study on isothermal redox-reactions for thermochemical energy storage was the combination of low-temperature oxidation of CoO at around 500 °C under increased O_2-pressure. The isothermal oxidation under varied oxygen contents at ambient pressure was selected as a starting point. In order to compare the reactivity towards O_2 in the desired temperature regime, samples of CoO were oxidized at 500, 520 and 550 °C using an atmosphere with 21 % O_2 (synthetic air) and 100 % O_2.

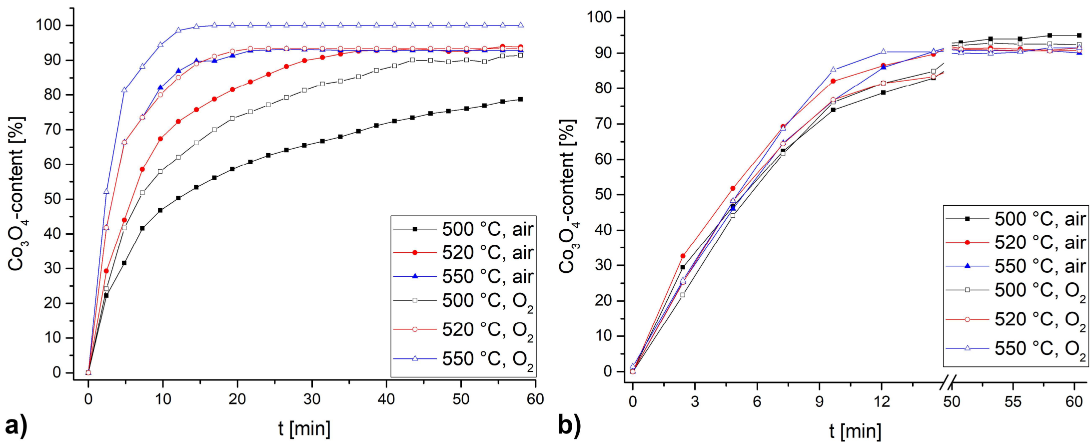

Fig. 2: Oxidation rate of CoO at several temperatures and O_2-concentrations for a) a CoO-sample obtained from thermal decomposition of Co_3O_4 under N_2 b) a commercial CoO sample

A concentrating plot of the different oxidation rates for CoO – obtained from Co_3O_4 by thermal reduction of the material under N_2 at 890 °C for 5 minutes – is shown in figure 2a. Especially for the series at 500 °C a notable difference in oxidation rate between the measurement under air and O_2 is found. The impact of the O_2 concentration with increasing temperature is superimposed by the thermal contribution, leading to a nearly identical oxidation rate observed in the experiments at 520 °C under O_2 and 550 °C under air.

In principle both a Co_3O_4 initially reduced to CoO and a CoO prepared on an industrial scale should be feasible for a Co-based TCES process. For comparison, the same series of oxidation experiments was repeated using a commercial sample of CoO (figure 2b). Interestingly, a completely different picture is observed in this case. The chemically identical sample provides much faster oxidation rates with conversions above 80 % under all applied conditions within the first 15 minutes. The reason for this behavior was found in the SEM-images of both precursors, showing for the Co_3O_4 (figure 3a) large sintered agglomerates, whereas the CoO (figure 3b) consisted of small, isolated particles. The different O_2-concentrations, as well as the various temperatures, have no impact on the initial particle morphology (see figure S2).

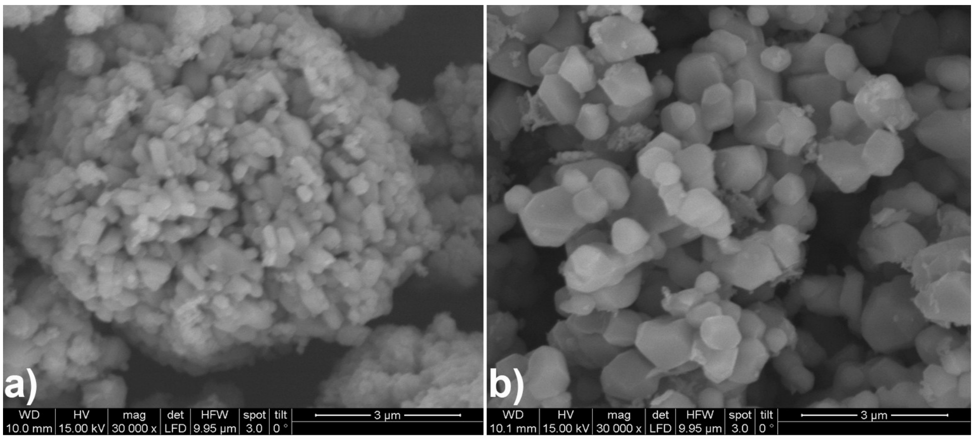

Fig. 3: SEM-images of a) commercial Co_3O_4 b) commercial CoO. Image size 9 x 9 µm

3.3 Isothermal oxidation of CoO under elevated O_2 pressure

In order to facilitate investigations on the impact of an increased oxygen pressure, which is higher than the atmospheric one, Co_3O_4 that has been *in-situ* reduced under N_2 was used for the experimental approach. Although, the commercial CoO sample would provide faster reaction rates, no reliable results would have been obtained even with a high-end laboratory P-XRD setup.†

The oxidation rates for the experiments under ambient pressure, 3 bar and 6 bar O_2‡ are shown in figure 4, which reveals a rate-enhancing effect of the increased O_2 pressure for all three temperature levels. Obviously, the largest influence on the oxidation is observed for 500 °C (figure 4a). By applying 3 bar O_2 the conversion within the first 15 minutes is enhanced about 20 %. 6 bar O_2 result in a quantitative Co_3O_4 formation after 30 minutes, the reaction rate being only slightly faster than for 3 bar.

In case of the series at 520 °C, O_2 oxidation under ambient pressure and 3 bar O_2 reveal only slight differences in the reaction rate. At 6 bar O_2 an increased oxidation within the first 6 minutes leads to quantitative Co_3O_4 formation after 15 minutes. Finally, at 550 °C the temperature increase predominates over the increased pressure, as both 3 bar and 6 bar O_2 yield a complete oxidation - 3 bar after 12 minutes, 6 bar after 8 minutes.

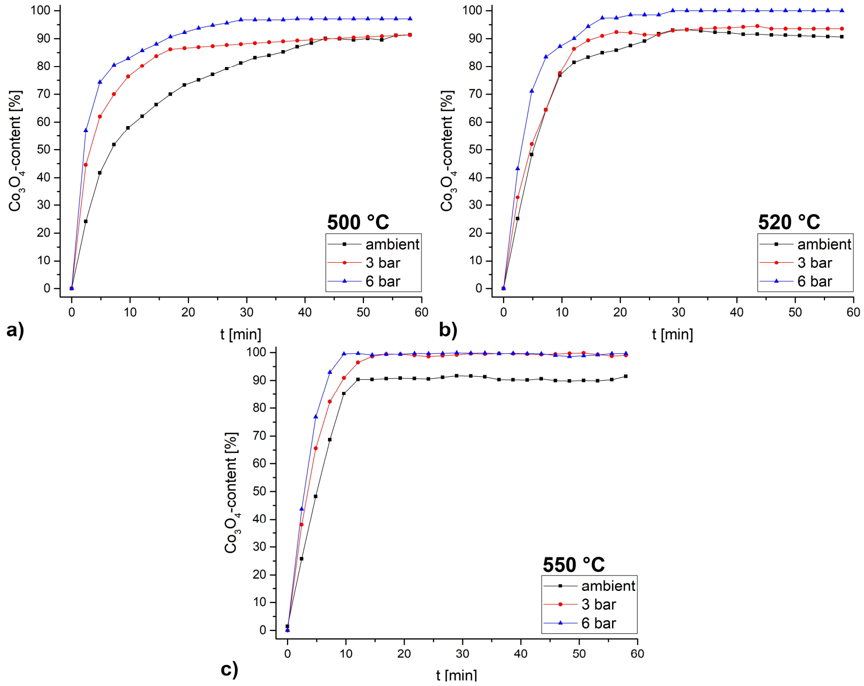

Fig. 4: Oxidation rate of CoO at different pressures and temperatures at a) 500 °C b) 520 °C c) 550 °C

Based on these results a lower oxidation temperature for CoO in a TCES-process seems feasible, increasing the reaction rate by moderately enhanced pressure. For technological processes elevated pressure is always correlated with much higher expenditures regarding the process design. Using only 6 bar O_2 – for all three temperatures yielding a notable enhancement of the conversion rate – may be still worth the efforts aiming for an oxide-based

† This limitation – also slightly affecting the accuracy of the phase-determination for the high Co_3O_4-contents – is attributed to the overlap of significant peaks in the diffractograms of the two Co-phases, as well as the high fluorescence of the Co-containing samples in combination with the available Cu K_α-radiation (see figure S3). To ensure the data quality, a minimum measurement time of 2 minutes per diffractogram was necessary.

‡ Although, the used Anton Paar XRK 900 would tolerate pressures up to 12 bar, applying a higher pressure than 6 bar O_2 extends due to radiation absorption and the fluorescence background the measurement time notably, so within one diffractogram the transformation from CoO to Co_3O_4 is completed. For similar measurements under higher pressures a different X-Ray source or a synchrotron would be needed.

medium-temperature TCES-process.

The only drawback of the increased pressure is the promoted sintering of the material, which is already evidenced in the SEM-images of the Co_3O_4 samples, oxidized at 550 °C and various pressures (see figure 5). Nevertheless, this changed particle morphology so far was not found to decrease the reactivity of the material on repeated cycling.

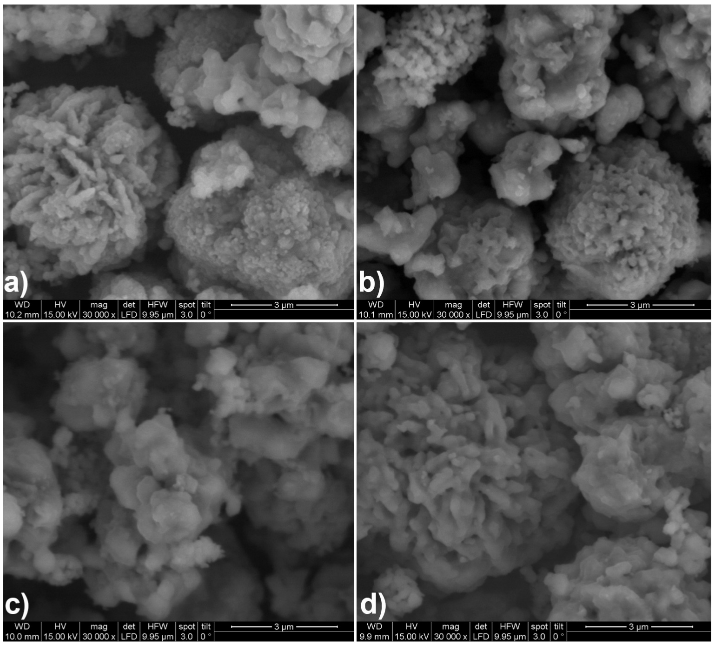

Fig. 5: Particle morphology of Co_3O_4 after oxidation at 550 °C and varied O_2 pressures a) Co_3O_4 starting material b) ambient pressure c) 3 bar O_2 d) 6 bar O_2. Image size 9 x 9 µm

3.4 Isothermal oxidation of Mn_3O_4

Similar to the study on the isothermal oxidation of CoO, a series was carried out also on Mn_3O_4 which was oxidized at different temperatures (470 °C, 500 °C, 520 °C, 550 °C) and ambient pressure under synthetic air and pure oxygen (figure 6).

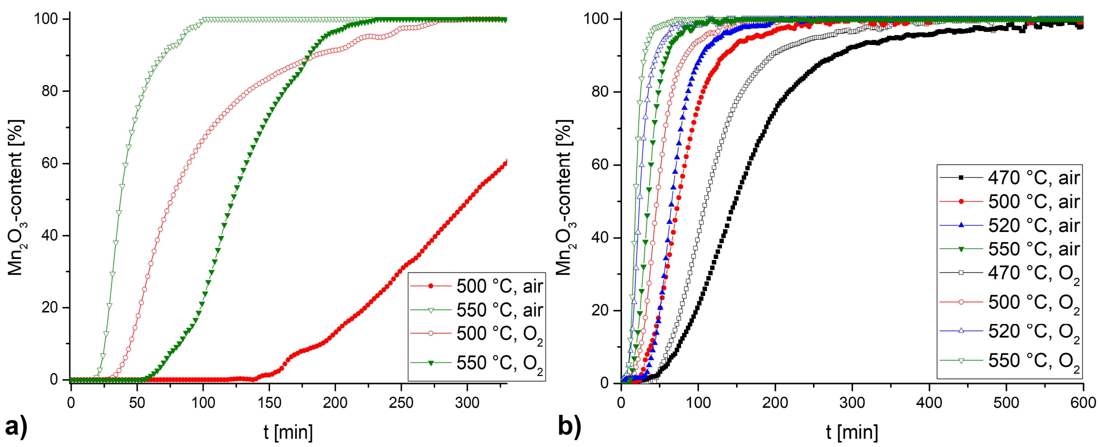

Fig. 6: Oxidation rate of Mn_3O_4 at various temperatures and O_2-concentrations for a) a Mn_3O_4-sample obtained from thermal decomposition of MnO_2 under N_2 b) a commercial Mn_3O_4 sample

Similar to the Co-system also for Mn_3O_4 a notable difference between the *in-situ* reduced sample under N_2 (figure 6a) and the commercially obtained Mn_3O_4 (figure 6b) was found. For the freshly reduced Mn_3O_4 at 500 °C under air within 330 minutes only 62 % of Mn_2O_3 are formed, whereas O_2 enables complete conversion to Mn_2O_3. Still a notable difference is observed at 550 °C, where both air and O_2 result in complete re-oxidation.

In the case of the commercial Mn_3O_4 a clear trend towards faster oxidation rates, both with increased temperature and O_2-content is found. Similar to CoO also for Mn_3O_4 temperature increases the oxidation rate more efficiently than a higher O_2 concentration. Comparable oxidation rates in this case are found at 550 °C under air and 520 °C under O_2.

4. Conclusion

In the present study the redox-couple Co_3O_4 / CoO was investigated with respect to an isothermal redox-cycle, triggered by changing the atmosphere from N_2 to O_2 between 880 – 920 °C. A reasonably linear correlation was found between the reduction / oxidation times and the applied temperature. Within the investigated temperature range the best conditions for an isothermal redox-cycle were found at 900 °C, as both reduction and oxidation take place quantitatively within 4.5 minutes. This represents an improvement of the so far reported results on isothermal cycling.

Based on former results an isothermal low-temperature oxidation of CoO between 500-550 °C under increased O_2-pressure was attempted, allowing for the application (only discharging) of a TCES-material featuring a high energy density at medium-temperatures. Increasing the O_2-pressure during oxidation from ambient conditions to 6 bar resulted in an attractive increase of reaction rate, discharging the CoO (oxidation to Co_3O_4) quantitatively at 500 °C within 24 minutes, at 550 °C within 8 minutes.

Elevated pressures during the oxidation process allow for a shift of the discharging reaction towards lower temperatures. This enables the application of the *per se* attractive high energy density of metal-oxide redox-reactions at temperatures, where they so far could not be operated, as the oxidation (discharging) required higher temperatures. This could be attractive for complementing an existing process with thermochemical energy storage, when pressurized air / oxygen is already available, or when a storage material with high energy density and a fast reaction rate is required at lower temperatures.

Mn_3O_4 was found to be too slow in its oxidation under all investigated conditions to be competitive in comparison to CoO.

5. References

1. Dinker, A., M. Agarwal, and G.D. Agarwal, 2015. Heat storage materials, geometry and applications: A review. Journal of the Energy Institute
2. Zalba, B., et al., 2003. Review on thermal energy storage with phase change: materials, heat transfer analysis and applications. Applied Thermal Engineering 3, 251-283.
3. Ali H. Abedin, M.A.R., 2011. A Critical Review of Thermochemical Energy Storage Systems. The Open Renewable Energy Journal 42-46.
4. Cot-Gores, J., A. Castell, and L.F. Cabeza, 2012. Thermochemical energy storage and conversion: A-state-of-the-art review of the experimental research under practical conditions. Renewable and Sustainable Energy Reviews 7, 5207-5224.
5. T. Yan, R.Z.W., T. X. Li, L.W.Wang, Ishugah T. Fred, 2015. A review of promising candidate reactions for chemical heat storage. Renewable and Sustainable Energy Reviews 13-31.
6. van Essen, V.M., et al., 2009. Characterization of Salt Hydrates for Compact Seasonal Thermochemical Storage. 825-830.
7. Knoll, C., et al., 2017. Probing cycle stability and reversibility in thermochemical energy storage – $CaC_2O_4{\cdot}H_2O$ as perfect match? Applied Energy 1-9.
8. Pardo, P., et al., 2014. A review on high temperature thermochemical heat energy storage. Renewable and Sustainable Energy Reviews 591-610.
9. Agrafiotis, C., et al., 2014. Exploitation of thermochemical cycles based on solid oxide redox systems for thermochemical storage of solar heat. Part 1: Testing of cobalt oxide-based powders. Solar Energy 189-211.
10. Agrafiotis, C., et al., 2016a. Exploitation of thermochemical cycles based on solid oxide redox systems for thermochemical storage of solar heat. Part 5: Testing of porous ceramic honeycomb and foam

cascades based on cobalt and manganese oxides for hybrid sensible/thermochemical heat storage. Solar Energy 676-694.

11. Agrafiotis, C., et al., 2015a. Exploitation of thermochemical cycles based on solid oxide redox systems for thermochemical storage of solar heat. Part 2: Redox oxide-coated porous ceramic structures as integrated thermochemical reactors/heat exchangers. Solar Energy 440-458.
12. Agrafiotis, C., et al., 2015b. Exploitation of thermochemical cycles based on solid oxide redox systems for thermochemical storage of solar heat. Part 3: Cobalt oxide monolithic porous structures as integrated thermochemical reactors/heat exchangers. Solar Energy 459-475.
13. Karagiannakis, G., et al., 2016. Cobalt/cobaltous oxide based honeycombs for thermochemical heat storage in future concentrated solar power installations: Multi-cyclic assessment and semi-quantitative heat effects estimations. Solar Energy 394-407.
14. Babiniec, S.M., et al., 2015. Investigation of LaxSr1−xCoyM1−yO3−δ (M=Mn, Fe) perovskite materials as thermochemical energy storage media. Solar Energy 451-459.
15. Block, T., N. Knoblauch, and M. Schmücker, 2014. The cobalt-oxide/iron-oxide binary system for use as high temperature thermochemical energy storage material. Thermochimica Acta 25-32.
16. Liu, X. and C. Prewitt, 1990. High-temperature X-ray diffraction study of Co_3O_4: Transition from normal to disordered spinel. Physics and Chemistry of Minerals 2,
17. Carrillo, A.J., et al., 2014. Thermochemical heat storage based on the Mn_2O_3/Mn_3O_4 redox couple: influence of the initial particle size on the morphological evolution and cyclability. J. Mater. Chem. A 45, 19435-19443.
18. Alonso, E., et al., 2013. Kinetics of Mn_2O_3–$Mn_3O_4$and Mn_3O_4–MnO Redox Reactions Performed under Concentrated Thermal Radiative Flux. Energy & Fuels 8, 4884-4890.
19. Chen, S., et al., 2013. Synthesis of Mn_2O_3 microstructures and their energy storage ability studies. Electrochimica Acta 360-371.
20. Carrillo, A.J., et al., 2015. Improving the Thermochemical Energy Storage Performance of the Mn_2O_3/Mn_3O_4 Redox Couple by the Incorporation of Iron. ChemSusChem 11, 1947-1954.
21. Wokon, M., A. Kohzer, and M. Linder, 2017. Investigations on thermochemical energy storage based on technical grade manganese-iron oxide in a lab-scale packed bed reactor. Solar Energy 200-214.
22. Agrafiotis, C., M. Roeb, and C. Sattler, 2016b. Exploitation of thermochemical cycles based on solid oxide redox systems for thermochemical storage of solar heat. Part 4: Screening of oxides for use in cascaded thermochemical storage concepts. Solar Energy 695-710.
23. Möller, S. and R. Palumbo, 2001. The Development of a Solar Chemical Reactor for the Direct Thermal Dissociation of Zinc Oxide. Journal of Solar Energy Engineering 2, 83.
24. Muthusamy, J.P., N. Calvet, and T. Shamim, 2014. Numerical Investigation of a Metal-oxide Reduction Reactor for Thermochemical Energy Storage and Solar Fuel Production. Energy Procedia 2054-2057.
25. Carrillo, A.J., et al., 2016. Revisiting the BaO_2/BaO redox cycle for solar thermochemical energy storage. Phys. Chem. Chem. Phys. 11, 8039-8048.
26. Müller, D., et al., 2017. Combining in-situ X-ray diffraction with thermogravimetry and differential scanning calorimetry – An investigation of Co_3O_4, MnO_2 and PbO_2 for thermochemical energy storage. Solar Energy 11-24.
27. Degen, T., et al., 2014. The HighScore suite. Powder Diffraction S2, S13-S18.
28. http://www.icdd.com,

6. Appendix

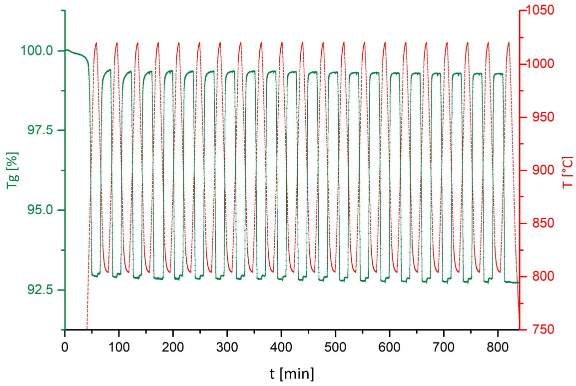

Fig. S1: 20 consecutive redox-cycles of Co_3O_4 under alternating atmosphere (N_2 vs. O_2)

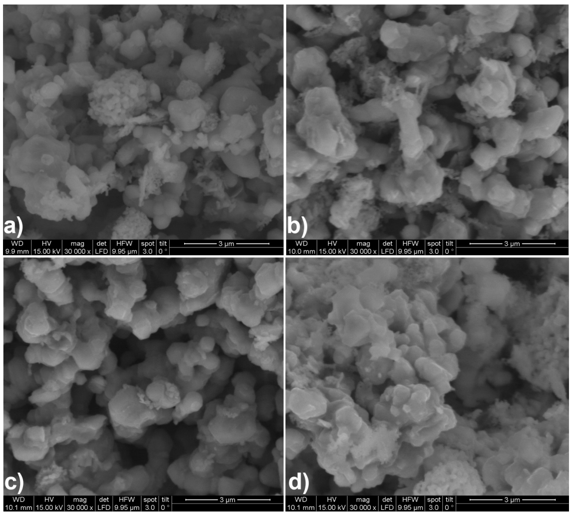

Fig. S2: SEM images of different Co_3O_4 samples after the oxidation in the P-XRD a) CoO after oxidation under air at 500 °C b) CoO after oxidation under air at 550 °C c) CoO after oxidation under O_2 at 500 °C d) CoO after oxidation under O_2 at 550 °C. Image size 9 x 9 µm

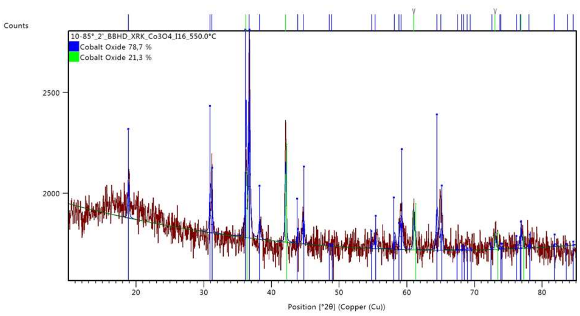

Fig. S3: P-XRD of a mixed CoO / Co_3O_4 sample, showing the moderate signal-to-noise ratio for the weaker peaks due to the X-Ray fluorescence of Co